Dynamic Point Selection CoMP Enabled Hybrid[1] Powered Green Cellular Networks

[1]Abu Jahid, [2]Abdullah Bin Shams and [3]Md. Farhad Hossain

[1]Department of Electrical, Electronic and Communication Engineering, Military Institute of Science and Technology, Dhaka-1216, Bangladesh

[2]Department of Electrical and Electronic Engineering, Islamic University of Technology, Gazipur-1704, Bangladesh

[3] Department of Electrical and Electronic Engineering, Bangladesh University of Engineering and Technology, Dhaka-1000, Bangladesh

Email: [1]setujahid@gmail.com, [2]abdullahbinshams@gmail.com, [3]mfarhadhossain@eee.buet.ac.bd

Abstract

Integration of renewable energy (RE) harvester has emerged as a long-term solution for the next generation cellular networks for reducing their operational expenditures and CO_2 footprints. However, the dynamic nature of RE generation could lead to energy outage and service quality deterioration. Thus, utilization of commercial grid supply in conjunction with RE generators is a more realistic option for sustainable network operations. Therefore, this article proposes an energy-efficient hybrid framework for achieving envisaged green cellular networks. Under the proposed framework, each base station is equipped with on-site solar energy harvester as the primary energy source along with the traditional grid electricity supplying additional energy demand. Afterward, dynamic point selection type coordinated multi-point transmission technique is integrated for selecting the best serving BS for a user. A comprehensive investigation is carried out in the context of downlink LTE-A cellular networks for evaluating energy efficiency performance of the proposed framework.

Index Terms

Energy harvesting; Energy efficiency; Coordinated Multi-point transmission; sustainable wireless networks; Hybrid power supply; green cellular networks.

1 INTRODUCTION

In recent years, the explosive growth of Information and Communication Technologies (ICT) has improved our lives enormously by offering different data-oriented services, such as multimedia communication, online gaming, high-quality video streaming, etc. With the increasing demand of diverse type of data requirements, cellular operators worldwide have been deploying base stations (BSs) at an enormous pace [1], [2]. The mass deployment of BSs worldwide is pushing the limits of energy consumption at an unprecedented

level in the networks. This remarkable inflation in energy consumption of cellular networks is exerting a tremendously detrimental impact on both the economic and the ecological implications, which is an alarming concern for cellular operators. Apart from the financial aspects, growing concerns on global warming due to the ever increasing carbon footprints has proliferated intensive attention in ICT sector. It is estimated that the energy consumption of ICT industry is expected to increase at a staggering rate by 150% from 20 TWh in 2011 to 50 TWh in 2020 and contribute about 2-4 % of total carbon emissions. The massive growth of energy consumption is forecasted to increase in future by a factor of 30 due to the immense growth of cellular data traffic [3], [4]. Therefore, with the escalating awareness of the aforementioned issues, green communications have drawn broad attention amongst the telecom regulatory bodies and have led to an emerging trend of addressing energy efficiency (EE).

To tackle the cumbersome energy consumption, exploiting green energy from renewable energy harvester (EH) is a promising supplementary solution. Rebewable EHs enable BSs to lower down the contribution to global warming by reducing the utilization of energy generated from fossil fuels. Recently, many cellular operators around the world are implementing renewable energy (RE) generators, such as photovoltaic (PV) solar panels, wind turbines and geothermal at their BSs to obtain clean and cheap energy [5], [6]. Despite the potential benefits of such approach, the inherent randomness of RE generation can severely degrade the system performance of large-scale cellular networks [7]. As a result, commercial grid electricity is still required to mitigate the variability of RE generation in order to maintain desired quality of service (QoS). Therefore, envisioning BSs to be powered by hybrid supplies combining RE sources with the traditional on-grid supply has become a promising alternative and provoked the current work.

1.1 Coordinated Multi-point (CoMP) Transmission Technique

In CoMP transmission, multiple BSs coordinate with each other in a way for delivering a better service for a user equipment (UE). CoMP has the potential to enhance throughput, coverage performance and overall spectrum efficiency (SE) [8]–[11]. Downlink CoMP can be categorized into three types as outlined by 3GPP - joint transmission (JT), dynamic point selection (DPS) and coordinated scheduling/coordinated beamforming (CS/CB) [8]. In JT technique, multiple coordinating BSs transmit data simultaneously to a single UE. Strong coordination and tight synchronization among JT BSs are required. Moreover, large amount of data need to be transferred among the BSs, which raise computational complexity as well as increased latency issues. On the other hand, in CS/CB technique, the signal is transmitted from only one BS. Scheduling decisions and details of UE beam forming are required to be coordinated among multiple BSs [9]. However, CS/CB faces the problems of poor fairness, high signaling overhead and less diversity gain [10]. Whereas, in DPS technique, user data is available at multiple BSs, but data can only be transmitted from a single BS at a time. Unlike the other CoMP techniques, tight synchronization is not required. A UE randomly select the best serving BS at each time interval. Also, no precoding scheme is involved in it. However, frequent handover of UEs can occur [11]. Thus, available CoMP techniques have their relative advantages and disadvantages. However, this paper focuses on the integration of DPS CoMP technique in hybrid powered long-term evolution - advanced (LTE-A) cellular networks for improving EE. Investigation on other CoMP techniques is currently going on in our other works and will be included in our future publications.

It is worthwhile to mention here that for proper operations of CoMP transmissions, it requires feedback from UEs as well as interaction among the coordinating BSs. For instance, accurate channel state information (CSI) is one such vital feedback, which includes a channel quality indicator (CQI), a precoding matrix indicator (PMI), and a rank indicator (RI) [12]. CQI, RI and PMI indicate the proper modulation coding scheme, the number of possible transmission layers and the best suitable precoding matrix respectively. Furthermore, the cooperating BSs need to exchange information in a synchronized manner. For instance, precise CQI

calculation requires the information on the interference situation of the cooperating BSs. On the other hand, there are two basic design issues in optimizing CoMP transmissions. The first one is the BS cluster formation (CF) problem, while the other one is the resource allocation (RA) problem for optimizing spectrum and power uses among multiple BSs within a cluster. All such operations involves a large amount of feedback signal among various entities in the network, which may exert significant overhead in the system.

1.2 Contributions

This paper proposes and investigates the potential of DPS CoMP transmission approach for improving the EE of hybrid power supply based cellular networks. The contributions of this paper are summarized as follows:

- A generalized hybrid energy usage framework is developed for future cellular BSs for reducing on-grid energy consumption. A BS under the proposed framework includes renewable EH PV solar modules with batteries for energy storage as well as a connection to the commercial electricity grid to be used as the secondary energy source. Proposed hybrid energy usage model is then broadly analyzed integrating DPS CoMP technique for further improvement of EE.
- We extend the proposed model for multi-cell scenario considering the tempo-spatial behavior of both RE generation and traffic profile. Some limiting parameters of network performance, including inter-cell interference (ICI), log-normal shadow fading and load-dependent BS power consumption models are also considered.
- Extensive simulations are carried out for investigating the network performance in terms of EE, energy consumption index (ECI) and energy consumption gain (ERG) under different system parameters including solar generation capacity and battery state of charge. Afterward, the proposed system performance is compared with the existing non-CoMP based hybrid scheme and the conventional scheme.

The remainder of this paper is organized as follows. In section 2, we first present a thorough study of the related works. Section 3 describes the proposed hybrid powered cellular network model along with solar energy generation and storage models, BS energy consumption model and UE-BS association policy. Performance metrics are outlined in Section 4. Simulation setup and the simulation results with insightful analysis are presented in section 5. Finally, the paper is concluded in section 6 by summarizing the key findings.

2 Related Works

With the growing awareness of global warming and financial consequences of increasing energy consumption, cellular operators as well as vendors are highly concerned for seeking a way to improve EE in their networks [13]–[15]. BSs in radio access networks (RAN) are the most energy consuming equipment amounting around 60-80% of total consumption [16], [17]. Therefore, the subject of energy efficiency in RAN infrastructures, mainly in BSs, has become the center of focus to the researchers from both academia and industry.

A promising solution is to exploit RE sources, such as solar energy and wind energy for powering BSs with cheap and clean energy. With the advancement of green energy technologies, RE has shown to yield significant reductions in operational costs and carbon footprint for cellular operators by reducing traditional grid consumption. There exists few works on the energy-efficient solutions for cellular networks using hybrid energy supplies for BSs [18], [19]. In [18], authors studied the on-grid energy minimization in green heterogeneous networks considering the temporal and spatial dynamics of mobile traffic and green energy generation. Authors in [19]

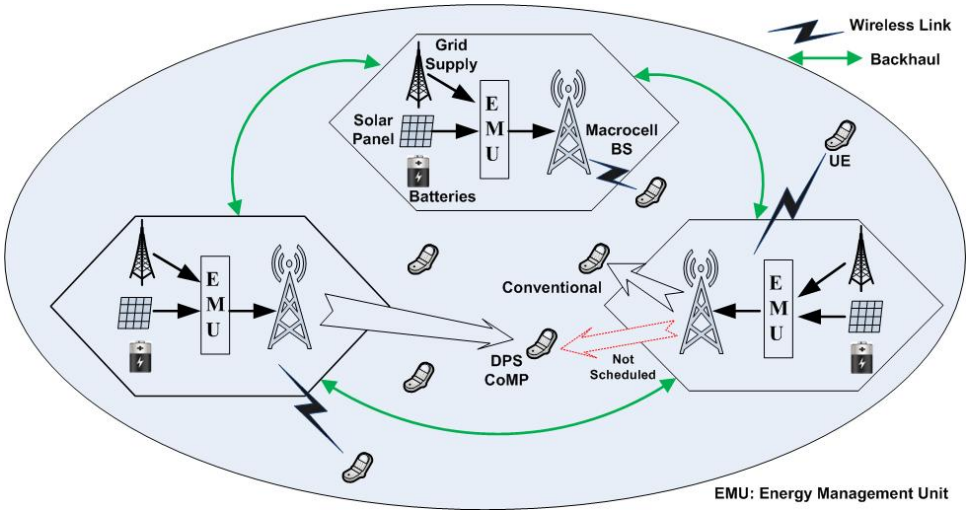

Fig. 1: A Section of the proposed cellular network model with hybrid power supply.

formulated the minimization of the total energy consumption cost considering the variation between the realistic and practical traffic distribution.

An effective scheme for improving EE as well SE is the incorporation of CoMP transmission technique in wireless networks [12], [20]. For instance, authors in [12] proposed a QoS priority-based coordinated scheduling and hybrid spectrum access scheme for downlink CoMP transmission in two-tier heterogeneous networks. The proposed method can achieve outstanding cell-edge throughput performance and reduce the call blocking. Whereas, [20] presented an energy-aware cooperation among BSs for enhancing SE under CoMP based green cellular networks without considering the tempo-spatial nature of solar generation. On the other hand, very few works have been carried out in the context of CoMP enabled hybrid powered green cellular networks [21], [22]. Performance of JT CoMP enabled LTE-A cellular networks with hybrid supplies was thoroughly investigated in [21]. Energy harvesting technology with CoMP transmission in cellular communications based on joint energy and communication cooperation over smart grid was analyzed in [22]. Resulting scheme is shown to be capable to substantially improve the downlink throughput compared to the sub-optimal designs without communication and/or energy cooperation. In addition, [23] developed a CoMP based simulator for the green powered LTE-A cellular networks addressing the above issues, which offers a free license for academic research and non-commercial use.

3 System Model: Components, User Associations and Network Operations

This section presents the proposed cellular network model along with various features in the context of orthogonal frequency division multiple access (OFDMA)-based LTE-A cellular systems.

3.1 Network Layout

We consider the downlink of a multi-cell cellular network comprising a set of N macrocell BSs $\mathbb{B} = \{\mathcal{B}_1, \mathcal{B}_2, ..., \mathcal{B}_N\}$ and covering an area $\mathcal{A} = \{\mathcal{A}_1 \cup \mathcal{A}_2 \cup ... \cup \mathcal{A}_N\} \subset \mathbb{R}^2$. Here, $\mathcal{A}_i$ is the coverage area of BS $\mathcal{B}_i$, $\forall i \in \{1, ..., N\}$. Macro BSs are assumed to be deployed using omnidirectional antennas in hexagonal grid fashion. Orthogonal frequency bands are allocated in a BS leading to zero intra-cell interference. On the other hand, universal frequency reuse is considered resulting in inter-cell interference.

All the macro BSs in the proposed network are powered by hybrid supplies, more specifically, a combination of PV solar energy and commercial on-grid energy. Each individual BS is equipped with on-site solar energy harvester, energy storage device, such as a

battery bank and a energy management unit (EMU). The EMU allows the integration of multiple energy sources and provides advanced energy management feature. Here PV solar modules is proposed as the primary energy source in order to ensure maximum utilization of green energy. Each BS is also connected to traditional grid that enables each BS to meet its energy deficit by utilizing grid electricity. We also propose to integrate DPS CoMP transmission technique for choosing the best serving BS for any UE. A schematic diagram of the network layout with hybrid supplies is depicted in Fig. 1. Furthermore, any BS during off traffic hours are switched into low power sleep mode for saving energy.

3.2 Link Model

This paper assumes a realistic channel model with log-normally distributed shadow fading. For a separation d between transmitter and receiver, path-loss in dB can be expressed as

$$PL(d) = PL(d_0) + 10\alpha log(\frac{d}{d_0}) + X_\sigma \tag{1}$$

where $PL(d_0)$ is the path-loss in dB at a reference distance d_0 and α is the path-loss exponent. $PL(d_0)$ can be calculated using the free-space path-loss equation. X_σ is the amount of shadow fading modeled as a zero-mean Gaussian random variable with a standard deviation σ dB.

Thus, the received power in dBm for k^{th} UE at a distance $d = d^{i,k}$ from i^{th} BS $\mathcal{B}_i$ is given by

$$P_{rx}^{i,k} = P_{tx}^{i,k} - PL(d) \tag{2}$$

where $P_{tx}^{i,k}$ is the transmitted power in dBm. The transmit power $P_{tx}^{i,k}$ from $\mathcal{B}_i$ to UE k satisfies $\sum_k P_{tx}^{i,k} \leq P_i^{max}$, where P_i^{max} is RF output power of BS $\mathcal{B}_i$ at its maximum traffic load.

On the other hand, inter-cell interference can be expressed as

$$\mathcal{I}_{k,inter} = P_{inter}^{i,k} = \sum_{m \neq i} (P_{rx}^{m,k}) \tag{3}$$

Then the received SINR $\gamma_{i,k}$ at k^{th} UE from BS $\mathcal{B}_i$ can be given by

$$\gamma_{i,k} = \frac{P_{rx}^{i,k}}{\mathcal{I}_{k,inter} + \mathcal{P}_N} \tag{4}$$

where $\mathcal{P}_N$ is the additive white Gaussian noise (AWGN) power given by $\mathcal{P}_N = -174 + 10log_{10}(\Delta f)$ in dBm with Δf is the bandwidth in Hz.

3.3 Solar Energy Generation Model

Daily solar energy generation profile is unpredictable, intermittent, and dynamic over time and space. In addition, harvested green energy depend on several sophisticated factors, such as temperature, solar light intensity, panel materials, generation technology and the geographic location of BS. We assume quasi-static time-slotted models for renewable energy harvesting rate that remain constant in each slot and may change from one slot to another. Thus, RE generated at $\mathcal{B}_i$, $i \in \{1, ..., N\}$ during time slot n is modeled as a random variable denoted by $r_i(t) \in [0, {r_i}^{max}]$, where ${r_i}^{max}$ is maximum available solar energy generation by $\mathcal{B}_i$. Green power generation can be defined as $\int_{(n-1)\tau}^{n\tau} b_i(t)dt = r_i(t)$, where $b_i(t)$ is obtained from the instantaneous solar power profile as depicted

TABLE 1: Solar panel and storage device parameters

Parameters	Type (Value)
Solar module type	Photovoltaic (Distributed)
Generation technology	CSP PV cell
Solar panel capacity	1 kWdc
DC to AC ratio	0.9
Array type	Fixed roof mount
Tilt	20 degrees
Azimuth	180 degrees
Storage type	Lead-acid battery (FLA-VRLA)
Storage capacity	2000 Wh
Storage factor	0.95

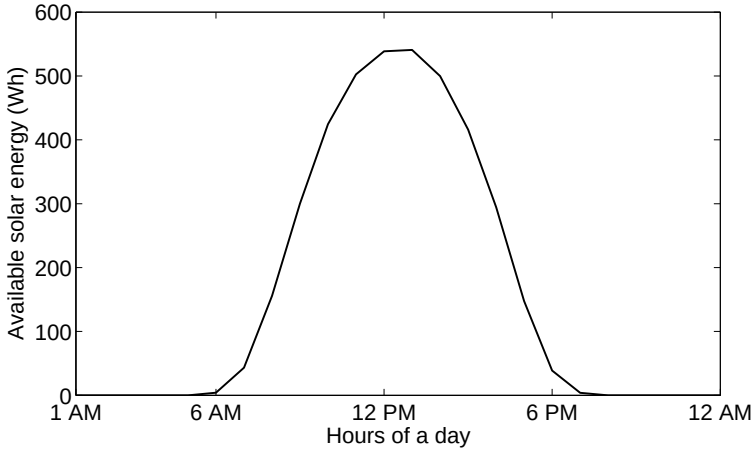

Fig. 2: Average hourly solar energy generation for Dhaka city of Bangladesh.

in Fig. 2 and τ is the duration of each time slot. Hence, this energy quantities represent the temporal averages over the corresponding time slots. The time varying average solar energy generation, $\bar{r_i}(t)$ is characterized by the following model [1]

$$\bar{r_i}(t) = \frac{{r_i}^{max} exp^{-(n-\beta_i)^2}}{\delta_i^2}\tau \tag{5}$$

In this model, β_i represents the position in time of the peak generation chosen to be noon, i.e., 12 hours, $\forall i \in \{1, ..., N\}$, δ_i indicates the shape width at half maximum of the peak, chosen to be 3 hours, $\forall i \in \{1, ..., N\}$, and the time duration of each slot τ is one hour.

Average hourly solar energy generation profile for full year in Dhaka city of Bangladesh is shown in Fig. 2. Here, solar energy profile for a particular region is estimated by adopting System Advisory Model (SAM) [24]. The curve indicates that the green energy generation starts at around 6:00 AM, reaches peak value at noon and fall down at zero level about 6:00 PM. SAM supports various solar power generation technologies. However, without losing the generality, distributed type concentrated solar power (CSP) PV technology with 1 kW solar panel is used for generating the shown curve. Parameters of the solar generation and storage systems for the considered solar module are summarized in Table 1.

TABLE 2: Summary of the notations used in the algorithms

$\mathcal{RB}_t$	Total number of LTE resource block (RB)
Δf	Bandwidth per RB (180 kHz for LTE)
$\chi_{i,j}$	Traffic load of BS $\mathcal{B}_i$ in j^{th} hour
μ	Storage factor
N	Total number of BSs
$P_{in}^{i,j}$	Total input power required for BS $\mathcal{B}_i$ in j^{th} hour
P_{sleep}	Power consumption of BS $\mathcal{B}_i$ in sleep mode
U	Total number of UEs
r	Solar energy generation
s_{max}	Maximum storage capacity
$s_{i,j}$	Nominal storage capacity of BS $\mathcal{B}_i$ in j^{th} hour
$d_{k\forall N}$	Distance of k^{th} UE from all N BSs
$\gamma_{k\forall N}$	Received SINR at k^{th} UE from all N BSs
T_j^{DPS}	Throughput for DPS CoMP scheme on j^{th} hour

3.4 Solar Energy Storage Model

In general, solar powered BSs possess battery bank to store excess electricity for the future consumption during periods without sufficient solar energy, such as at night and adverse weather condition. The battery characteristics, e.g., battery bank capacity, battery voltage, depth of discharge, lifetime and efficiency play vital roles in designing hybrid powered wireless networks. Depth of discharge (B_{DOD}), which refers to the percentage of energy that can be delivered, has an significant impact on the lifetime of a battery. Typically, the nominal capacity of a battery bank is the maximum state of charge of a battery, while the minimum state of charge of the battery ($B_{SOC_{min}}$) defines the threshold limit of battery charge level. B_{DOD} can be computed based on the following equation [6]

$$B_{DOD} = (1 - \frac{B_{SOC_{min}}}{100}) \tag{6}$$

However, various battery types, such as Nickle-cadmium (Ni-Cd), Nickel metal hydride (Ni-MH), Lithium-polymer, Lithium-ion, lead-acid, etc. are used in solar powered cellular BSs. Among the existing battery technologies, lead-acid battery is mostly preferred in solar powered BSs because of their lower cost and reliability [6]. During operation, storage devices keep charging and discharging according to the pattern of solar generation and BS consumption. The stored green energy at $\mathcal{B}_i$ is determined by the green energy consumption and generation of the previous time slot. For the proposed system, the amount of residual green energy $s_i(t)$ of BS $\mathcal{B}_i$ at time t can be given by [16]

$$s_i(t) = \mu s_i(t-1) + r_i(t) - d_i(t) \tag{7}$$

where r_i is the harvested green energy from PV solar panel and d_i is the energy demand of the BS. $0 \leq \mu \leq 1$ is the storage factor, i.e., the percentage of storage energy retained after a unit period of time. For example, $\mu = 0.9$ indicates that 10% energy will be lost in the storage during the time interval. It is to be noted that the stored energy can not exceed the maximum storage capacity. Therefore, if the generation is higher than the storage capacity, that amount of energy is considered as wastage.

Net renewable energy available at BS $\mathcal{B}_i$, denoted by $N_i(t)$, is the difference between RE generation and BS demand. That is $N_i(t)$

TABLE 3: Solar energy storage principle

1:	Initialize: P_{sleep}, s_{max}, μ, r, $s_{i,j}$, $\chi_{i,j}$
2:	Set initial storage s_i = 0
3:	Calculate P_{in}
4:	**for** j = 1 : τ : 24
5:	**for** $i = 1 : N$
6:	**if** $s_{i,j}$ + $r_j \geq s_{max}$
7:	$s_{i,j}$ = s_{max}
8:	**else**
9:	$s_{i,j}$ = $s_{i,j}$ + r_j
10:	**end if**
11:	**if** $s_{i,j} \geq P_{in}^{i,j}$
12:	$s_{i,j+1}$ = μ ($s_{i,j}$ - $P_{in}^{i,j}$)
13:	$P_{in}^{i,j}$ = 0
14:	**else**
15:	$P_{in}^{i,j}$ = $P_{in}^{i,j}$ - $s_{i,j}$
16:	$s_{i,j+1}$ = 0
17:	**end if**
18:	**end for**
19:	**end for**

= $r_i(t)$ - $E_i(t)$. This quantity can be positive or negative. Positive quantity representing a surplus energy available whereas negative quantity implies a deficit. The net energy consumption in a cooperative region may be partially nullified by the harvested green energy. The traditional grid energy will be used to fulfill the deficit whenever the green energy is inadequate. Under the proposed model, the green energy utilization and on-grid energy consumption of $\mathcal{B}_i$ under different scenarios are as follows:

Case I: If $s_i(t) \geq d_i(t)$, then BS $\mathcal{B}_i$ will be served by its respective storage. Hence, no on-grid energy will be consumed. Total green energy left in the storage after fulfilling the demand of BS $g_i(t)$ can be expressed as

$$g_i(t) = s_i(t) - d_i(t) \tag{8}$$

Case II: If $s_i(t) < d_i(t)$, then BS $\mathcal{B}_i$ feeds itself from its remaining own storage, though it is not sufficient to fully meet the demand. Therefore, on-grid consumption is required in the absence of sufficient green energy storage. Thus, the conventional grid energy consumption $c_i(t)$ by $\mathcal{B}_i$ becomes

$$c_i(t) = d_i(t) - s_i(t) \tag{9}$$

Thus, after partially fulfilling the energy demand of a BS, remaining green energy in the storage becomes zero, i.e., $g_i(t) = 0$. Pseudo code of the solar energy storage principle of each BS is presented in Table 3.

3.5 BS Power Consumption Model

BSs, the prime equipment of RAN infrastructure, comprise of multiple transceiver (TRX) chains which comprise of power amplifiers, baseband unit, radio frequency small-signal transciever, DC-DC power supply and a cooling system. This paper considers a single TRX

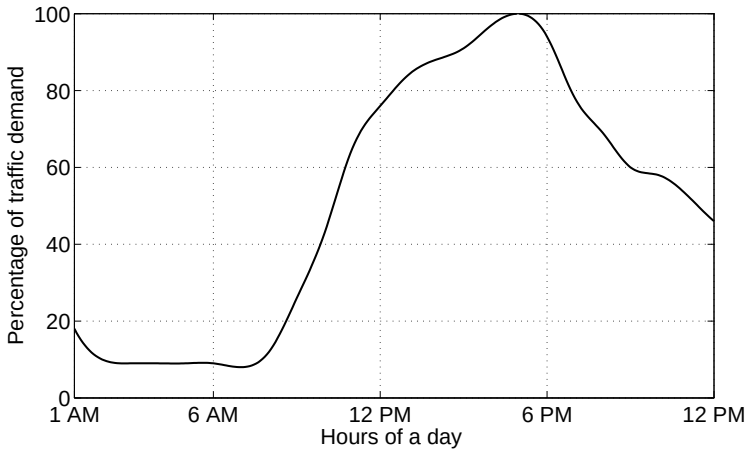

Fig. 3: Daily traffic load profile of a residential area.

chain for omnidirectional configuration. However, the power consumption of typical BSs directly varies with the respective traffic load, i.e., the number of active users. Similar to the solar energy generation, mobile traffic volume varies both in space and time domains.

Energy consumption of BSs can be sub-divided into two parts: the static energy consumption and the dynamic energy consumption. Total energy consumption in all the BSs in the network during a time slot of duration τ can be given by [25]

$$E_{in}(t) = \sum_{i=1}^{N} \{P_i^{act} y_i(t)\tau + P_i^{sleep}(1 - y_i(t))\tau\} + \sum_{i=1}^{N}\sum_{k=1}^{U} \Delta_i P_{tx}^{i,k}(t) x_{i,k}(t)\tau \tag{10}$$

where P_i^{act} and P_i^{sleep} account for the power consumption of BS $\mathcal{B}_i$ operating in active and sleep mode respectively, and Δ_i is the slope of load dependent power consumption of BS $\mathcal{B}_i$. Binary variable $x_{i,k}$ models the association between BSs and UEs as defined below.

$$x_{i,k} = \begin{cases} 1, & \text{if } k^{th} \text{ UE is served by } \mathcal{B}_i \qquad \forall i \in N, \forall k \in U \\ 0, & \text{otherwise} \end{cases} \tag{11}$$

On the other hand, the activity status of each BS is modeled by the binary variable y_i(t) such that

$$y_i = \begin{cases} 1, & \text{if } \mathcal{B}_i \text{ is active} \qquad \forall i \in N \\ 0, & \text{if } \mathcal{B}_i \text{ is in sleep mode} \end{cases} \tag{12}$$

Under the sleep mode operation, BSs switch to sleep mode from an active mode that are currently not serving any UEs. Typically, deactivating some hardware components can save energy consumption substantially since a great portion of energy is required to operate BSs in active mode. As a result, a reduced operational energy consumption is attributed whenever the sleep mode operation is applied. Now, by collecting terms, (10) can be reinterpreted as

$$E_{in}(t) = E^{dym}(t) + E^{sta} \tag{13}$$

where $E^{dym}(t)$ and E^{sta} represent the dynamic and static energy consumption of E_{in} respectively as presented below.

$$E^{dym}(t) = \sum_{i=1}^{N} \{P_i^{act} - P_i^{sleep}\} y_i(t)\tau + \sum_{i=1}^{N}\sum_{k=1}^{U} \Delta_i P_{tx}^{i,k}(t) x_{i,k}(t)\tau \tag{14}$$

TABLE 4: BS power consumption model parameters [14]

Parameters	Value
BS Type	Macro
η_{PA}	0.306
γ	0.15
$P_{BB}[W]$	29.4
$P_{RF}[W]$	12.9
σ_{feed}	0.5
σ_{DC}	0.075
σ_{MS}	0.09
σ_{cool}	0.1
Number of sectors, M_{sec}	1
Maximum transmit power, $P_{MAX}[dBm]$	43
$\triangle_p$	4.2
$P_{sleep}[W]$	54

$$E^{sta} = \sum_{i=1}^{N} P_i^{sleep} \tau \tag{15}$$

However, authors in [14] approximated the operating power of a BS as a linear function of RF output power P_{MAX} and BS loading parameter χ, which can be given by

$$P_{in} = \begin{cases} M_{sec}[P_1 + \triangle_p P_{MAX}(\chi - 1)], & \text{if } 0 < \chi \leq 1 \\ M_{sec} P_{sleep}, & \text{if } \chi = 0 \end{cases} \tag{16}$$

where the expression in the square brackets represents the total power requirement for a transceiver (TRX) chain, M_{sec} is the number of sectors in a BS and P_1 is the maximum power consumption in a sector. The load dependency is accounted for by the power gradient, $\triangle_p$. The loading parameter $\chi = 1$ indicates a fully loaded system, i.e., BS transmitting at full power with all of their LTE resource blocks (RBs) occupied and and $\chi = 0$ indicates idle state. Furthermore, a BS without any traffic load enters into sleep mode with lowered consumption, P_{sleep}. Now P_1 can be expressed as below [14]

$$P_1 = \frac{P_{BB} + P_{RF} + P_{PA}}{(1 - \sigma_{DC})(1 - \sigma_{MS})(1 - \sigma_{cool})} \tag{17}$$

where P_{BB} and P_{RF} are the power consumption of basedband unit and radio frequency transceiver respectively. Losses incurred by DC-DC power supply, mains supply and active cooling can be approximated by the loss factors σ_{DC}, σ_{MS} and σ_{cool} respectively. However, power consumption in the power amplifiers is represented by P_{PA} which depends on the maximum transmission power and power amplifier efficiency η_{PA} and can be given as follows [14]

$$P_{PA} = \frac{P_{MAX}}{\eta_{PA}(1 - \sigma_{feed})} \tag{18}$$

BS power consumption model parameters used in this paper are summarized in Table 4.

TABLE 5: UE association algorithm for DPS CoMP based network

1:	Initialize: $\mathcal{RB}_t$, $\chi_{i,j}$, $k \in 1, 2, ...U$
2:	**for** $j = 1 : \tau : 24$
3:	**for** $i = 1 : N$
4:	**if** $\chi_{i,j} \neq 0$ then
5:	Location of $U = \chi_{i,j}\mathcal{RB}_{tot}$ associated with $\mathcal{B}_i$ are updated
6:	**for** $k = 1 : U$
7:	Compute $d_{k\forall N}$ and $\gamma_{k\forall N}$
8:	Sort $\gamma_{k\forall N}$ in descending order
9:	Associate k^{th} UE to the BS providing the maximum SINR
10:	T_j^{DPS} = T_j^{DPS} + $\Delta f \log_2$ (1+$\gamma_{i,k}$)
11:	Update $\chi_{i,j}$
12:	**end for**
12:	**end if**
13:	**end for**
14:	**end for**

3.6 User Association Policy

In a conventional system, a UE is associated with the closest serving cell for communication which does not always ensure the best connection because of the randomness of shadow fading. On the other hand, a CoMP-enabled UE receives the better signal quality (i.e., improved SINR) and hence exhibits superior performance. A DPS CoMP technique has been adopted throughout this paper. In a network deployed with DPS CoMP based transmission technique, the BS providing the best SINR among the multiple coordinated BSs is dynamically selected for serving a UE. Pseudo code of the UE association policy is presented in Table 5.

4 Performance Metrics

4.1 Energy Efficiency (EE)

EE metric of a network given in terms of bits per joule can be defined as the ratio of the total throughput to the total power required for running the network. In this paper, we define the EE metric of the proposed network models with CoMP techniques and hybrid power supply as the ratio of the aggregate throughput of the network to that of the net on-grid power consumed by the network. Total achievable throughput in a network at time t with DPS CoMP can be calculated by Shanon's capacity formula as given below

$$R_{total}(t) = \sum_{k=1}^{U} \Delta f log_2(1 + \gamma_{i,k}), \text{ bps} \tag{19}$$

Thus the EE metric denoted as η_{EE} for time t can be written as

$$\eta_{EE}(t) = \frac{R_{total}(t)}{\sum_{i=1}^{N} P_g(i,t)}, \text{ bits/joule} \tag{20}$$

where $P_g(i,t) = P_{in}(i,t) - P_s(i,t)$ is the net grid power consumption, $P_{in}(i,t)$ is the total power demand and $P_s(i,t)$ is the solar power consumption in BS $\mathcal{B}_i$ at time t.

4.2 Energy Consumption Index (ECI)

An alternative performance metric for evaluating the EE of a BS is ECI, which can be given by [14]

$$ECI = \frac{P_{in}}{KPI} \tag{21}$$

where P_{in} refers to the total input power of a BS and KPI (Key Performance Indicator) indicates the total throughput of the BS. In other words, ECI is the reciprocal of EE and hence for the proposed networks, it can be evaluated by taking the inverse of (20). A lower value of ECI implies better EE and vice versa. ECI is more suitable for better visualization of network behavior when the denominator of (20) becomes zero.

4.3 Energy Consumption Ratio (ECR)

ECR is an equipment level metric, which is the ratio of energy consumption to the effective system capacity given in Watt/bps. Thus, ECR quantifies the amount of power required for transmitting one bit of information. A system with a lower ECR is more energy efficient in its energy usage as each bit consumes less power for data transmission.

4.4 Energy Consumption Gain (ECG)

ECG in green cellular communications can be defined as a ratio of the ECR metrics of the two systems under consideration. For example, if a hybrid powered cellular network without CoMP mechanism is taken as a baseline reference system, then by using ECG metric, we can measure the energy consumption improvement by our proposed DPS CoMP enabled hybrid system compared to the baseline system [21].

5 Performance Analysis

5.1 Simulation Setup

This section analyzes the performance of the proposed cellular network framework. A thorough investigation on the simulation results of different performance metrics is critically discussed. A MATLAB based Monte-Carlo simulation method is used in order to evaluate the system performance and results are calculated by averaging over 10,000 independent iterations. The network is deployed using a hexagonal grid layout of BSs equipped with omnidirectional antennas. Simulations are done considering inter-cell interference contributions made by the BSs placed in the two neighboring tiers surrounding the serving cell. We assume one RB for each associated UE. Once a RB is assigned to a UE, it remains dedicated to the UE and the UE continuously transmits data until the end of the call duration. That is, a circuit switch type application with a continuous data transmission is considered. We also assume same set of parameters for all BSs. Moreover, UEs are considered uniformly distributed over the geographical area. performance of the proposed network model for any non-uniform UE distribution can also be evaluated in a similar way. We also consider tempo-spatial diversities in both the renewable energy generation and traffic demand for the simulations. Unless otherwise specified, B_{DOD} =100% is considered for the simulations. A summary of the system parameters of the simulated network is set in reference to the LTE standard [8] as summarized in Table 6.

TABLE 6: Simulation parameters

Parameters	Value
Resource block (RB) bandwidth	180 kHz
System bandwidth,	10 MHz (50 RBs), 600 subcarriers
Carrier frequency, f_c	2 GHz
Duplex Mode	FDD
Cell radius	1000 m
BS Transmission Power	43 dBm
Noise power density	-174 dBm/Hz
Number of sectors, M_{sec}	1
Reference distance, d_0	100m
Path loss exponent, n	3.574
Shadow fading, σ	8 dB
Access technique, DL	OFDMA
UE distribution	Uniformly distributed

5.2 Result Analysis

Fig. 4 illustrates the average green energy utilization and on-grid consumption to run a BS of a cellular network under the proposed network model. The BS in consideration always tends to run entirely in solar energy if there is sufficient energy stored in the batteries. Since solar energy can only be generated during the day time, at night and morning, green energy is not enough to maintain QoS and hence conventional grid energy is needed to be drawn from the conventional grid. Typically, solar energy generation reaches its peak at noon and keeps the green energy storage healthy enough. Due to the temporal dynamics of sunlight, the available solar energy cannot always guarantee sufficient energy supply to fully operate a BS. In such cases, a BS is powered by on-grid energy to meet its associated users in order to avoid an outage. As observed, until 6 AM, a BS is fully run by on-grid supply. With the increase of solar energy generation, grid energy consumption rapidly falls down to zero level when there is adequate solar energy generation to fulfill the BS demand. During 8 AM to 8 PM, a BS satisfies its demand from its own solar energy and stores the surplus energy for future use. It can be readily identified that 100% on-grid energy savings can be achieved for a prolonged period of time under the proposed network model. As we advances to midnight, stored solar energy decreases gradually with the diminishing sunlight and once again on-grid energy is required to serve its associated users. Therefore, it can be safely inferred that the maximum utilization of green energy inherently reduces considerable amount of on-grid energy consumption.

A comparison of throughput performance over a day of the proposed network model integrating DPS CoMP with that of the 'Hybrid without CoMP' scheme is presented in Fig. 5. From the figure, it is clearly observed that throughput curve apparently follows the given traffic pattern as depicted in Fig. 3. A clear distinction of throughput performance is observed during the low traffic and peak traffic arrivals. During peak traffic periods, a higher number of RBs are allocated to the users resulting in higher throughput and vice versa. On the other hand, the proposed network model achieves a better throughput performance over the hybrid without CoMP system. This is because, total throughput is a function of the received signal quality. Under the DPS CoMP based hybrid cellular network model, UEs receive the best SINR resulting in a higher throughput as clearly evident from the figure. Moreover, throughput gap is more significant between the two hybrid systems during high traffic demands.

A comparison of the proposed network model with two other network schemes in terms of the key performance metric EE over

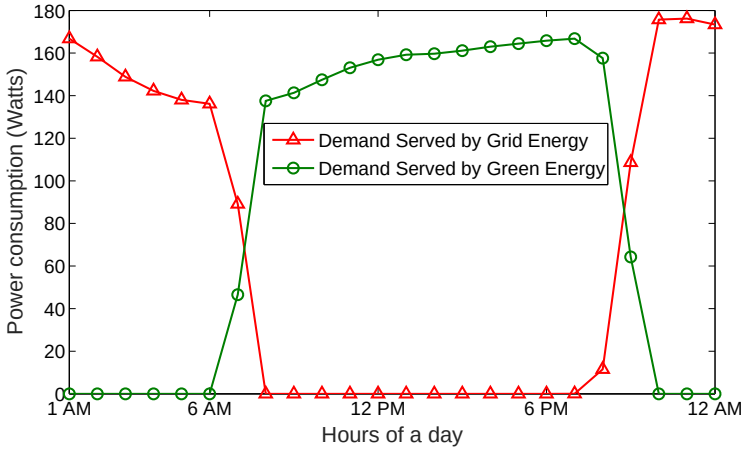

Fig. 4: Energy demand served by green energy source and on-grid supply.

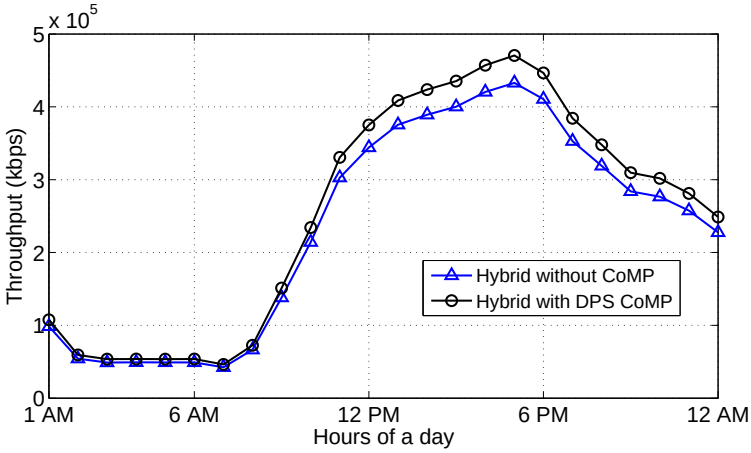

Fig. 5: Throughput comparison of a single BS between two different hybrid models.

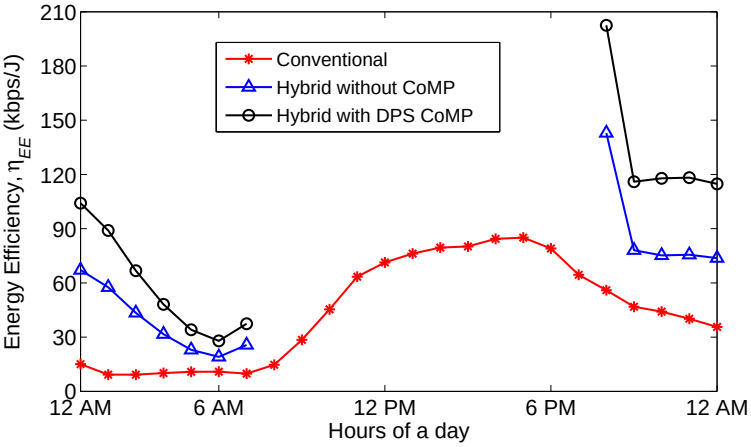

Fig. 6: Comparison of EE performance of the proposed model with other schemes.

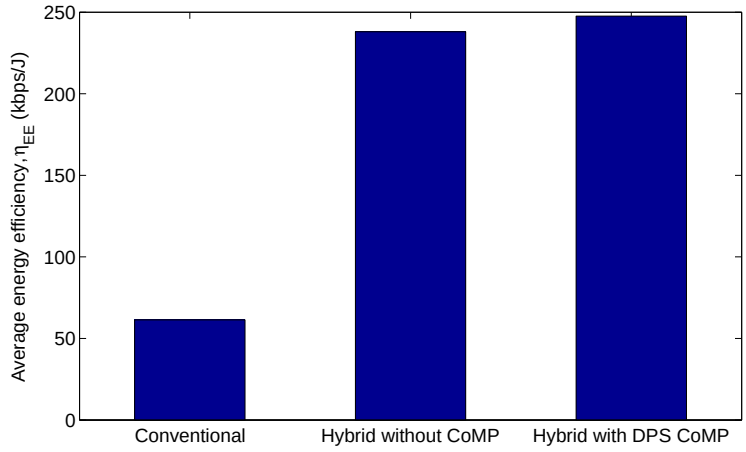

Fig. 7: A quantitive comparison of EE between two different hybrid schemes.

a period of a day is illustrated in Fig. 6. According to the definition, EE is linearly related to throughput. DPS CoMP based hybrid model provides the best SINR leading to the highest throughput and the best EE performance in turns as seen in the figure. However, EE curves for the both the hybrid schemes follow similar fashion. As observed, EE curve falls down during midnight to 6 AM due to the unavailability of solar energy and increased use of grid energy. As time passes, solar intensity increases with sun light availability (depicted in Fig. 2) leading to remarkably higher EE. With further green energy generation, EE reaches to infinity for a prolonged period implying that the BSs are mainly run by solar energy and do not consume grid energy to serve its associated users. This infinity EE region is marked by break lines in the figure. According to 20, net grid power requirement P_g goes to zero during 7 AM to 8:30 PM as the stored green energy is sufficient to supply full power demand of BSs and thus EE becomes infinity. After 8 PM, EE curve falls rapidly once again as the stored green energy becomes much lower for each BS and shows almost flatter response when storage is empty. The figure also includes the EE curve of the 'Conventional' network model showing inferior performance compared to our proposed network model. Here, the conventional scheme implies a system utilizing only traditional grid energy without any integration of RE sources and CoMP mechanism.

A detail quantitative comparison of the EE performance averaged over a day accounting the variability of solar energy generation and the tempo-spatial diversity of traffic arrivals is demonstrated in Fig. 7. As before, better throughput performance in DPS CoMP forces EE metric to be the highest for the proposed network model. It can be identified that the proposed network model attains substantially higher EE performance over the conventional scheme. On the other hand, proposed DPS CoMP enabled cellular system is also proved to be superior in terms of EE compared to the hybrid system without CoMP.

Fig. 8 presents the ECI metric over a day. As seen, ECI increases rapidly up to a certain point during low traffic hours and then starts to fall beyond that point. The up-trending nature of ECI curve signifies the relatively much higher grid energy consumption as the solar energy generation is not available. With the increase of solar intensity, ECI curve starts to move downward. Between 8 AM to 7 PM, ECI curve falls to zero implying zero on-grid energy consumption and hence ensure the maximum EE as explained beforehand. With diminishing sun light, stored energy drains out by powering the BSs and once again on-grid energy is required to supply the BSs resulting in an upward trend of ECI curve from 7 PM. Owing to better received signal quality, DPS CoMP enabled hybrid network model shows the superior ECI performance compared to the hybrid without CoMP system as clearly seen from the figure.

Fig. 9 illustrates the impact of the battery depth of discharge (B_{DOD}) on the ECI performance for the proposed hybrid with DPS

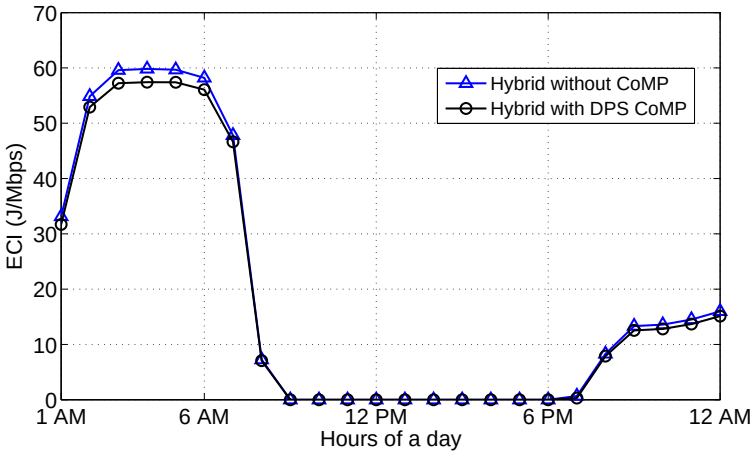

Fig. 8: ECI comparison between the proposed model and hybrid model.

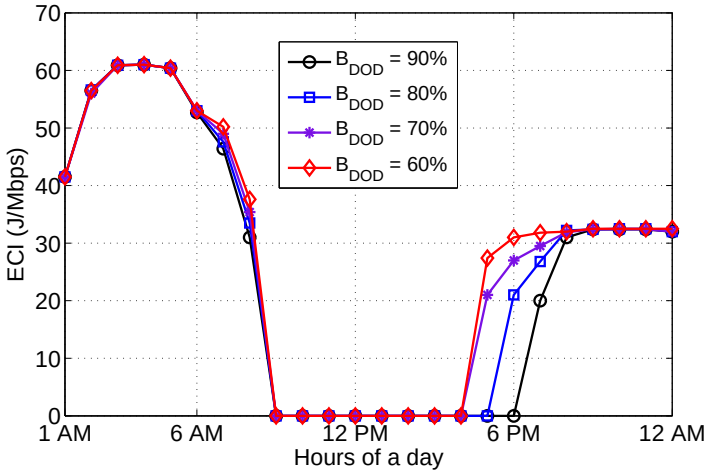

Fig. 9: Variation of ECI for the proposed model with different battery depth of charge.

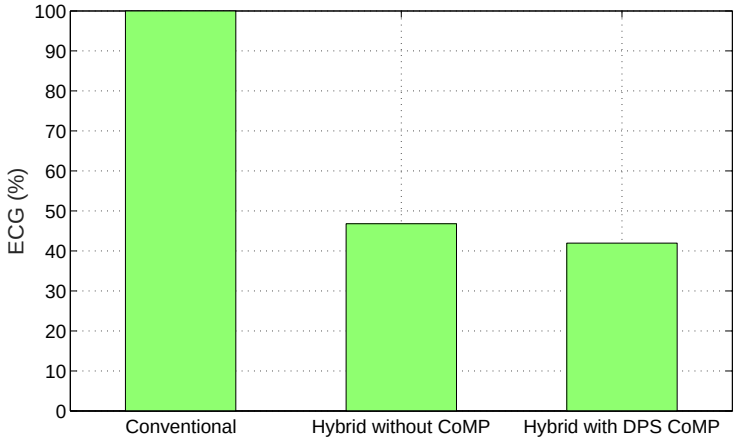

Fig. 10: ECG comparison between the hybrid models and conventional scheme.

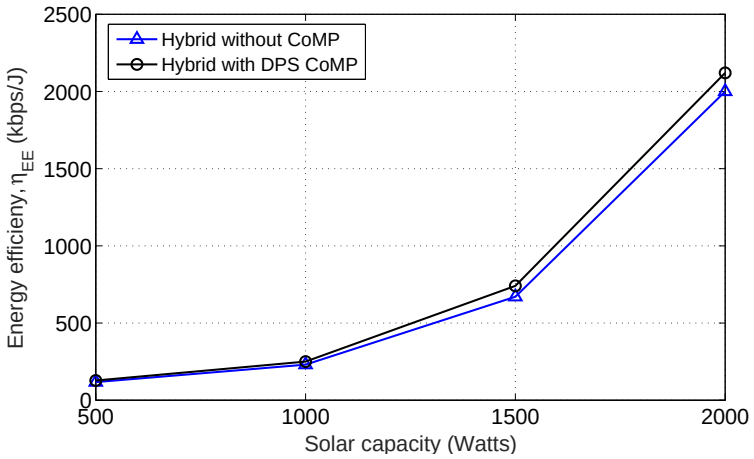

Fig. 11: EE variation of the prposed model with existing hybrid scheme with solar generation capacity.

CoMP enabled network model. Higher value of B_{DOD} implies better EE performance as higher amount of the stored energy is used to supply the BS load. For example, B_{DOD} = 90% indicates that 90% of the stored energy in the battery can be utilized. It is to be noted that all ECI curves in Fig. 9 follow the similar pattern as depicted in Fig. 8. The zero region in the curves has great significance. The wider zero region implies the lesser on-grid energy consumption and the battery bank can carry the BS demand for the more extended period. As expected, ECI metric curve for the B_{DOD} = 60% shows the inferior performance compared to others as the zero ECI zone is comparatively shorter.

A comparison of ECG performance metric of the proposed model with other schemes is demonstrated in Fig. 10. According to the definition of ECG in Section 4, it measures the energy consumption improvement relative to the reference baseline system. It is observed that DPS CoMP enabled hybrid system consumes about 59% and 6% less power compared to the 'Conventional' and the 'Hybrid without CoMP' traditional systems respectively. Therefore, the proposed hybrid cellular system is more energy efficient.

Finally, Fig. 11 demonstrates the impact of on-site solar module capacity on the EE performance of the proposed model. With the increment of installed solar panel capacity, storage capacity is also linearly scaled for guaranteeing no wastage of generated solar energy. As seen from the figure, EE of the hybrid network models shifts upward with the increment of solar capacity, which is mainly due to the increasing use of solar energy for running the BS. A large solar energy generation capacity may entirely phase out the consumption from the conventional grid supply attaining the maximum EE. Once again, EE performance of the proposed CoMP based system is found significantly better than that of the hybrid system without CoMP, which is more evident for higher solar generation capacity as illustrated in Fig. 11.

6 Conclusion

An energy-sustainable hybrid-powered framework for improving the energy efficiency performance of cellular networks has been proposed in this work. Base stations have been proposed to be connected to renewable energy source photovoltaic solar panel as well as conventional grid supply with a energy management system for reducing the consumption from the later one. Dynamic point selection type CoMP transmission technique has also been integrated for further improving energy efficiency. According to residual green energy, a Base station serves its associated users from solar energy until battery charge reached to a threshold level. A Base station is powered by grid energy only if there is a deficit of solar energy. Unlike most existing works, we have evaluated the system

performance considering the tempo-spatial diversities of both the renewable energy generation and traffic demand. Simulation results have shown that energy efficiency performance of the proposed hybrid scheme improves with the increment of the battery depth of discharge. Besides, a continuous improvement has been observed in the energy efficiency performance for the higher value on-site solar module capacity. Moreover, 100% on-grid energy saving has been found for a prolonged period of time. Furthermore, results have illustrated the potential of the proposed cellular network in substantially reducing the total energy consumption by over 59% and 6% respectively over the conventional and hybrid without CoMP schemes respectively. Future works will focus on the analytical modeling and the generalized algorithms for heterogeneous cellular networks considering all the CoMP techniques.

REFERENCES

[1] Farooq MJ, Ghazzai H, Kadri A, ElSawy H, Alouini MS. A Hybrid Energy Sharing Framework for Green Cellular Networks. IEEE Transactions on Communications. 2016 Dec; 65(2):918-34. https://dx.doi.org/10.1109/TCOMM.2016.2637917.

[2] Mahapatra R, Nijsure Y, Kaddoum G, Hassan NU, Yuen C. Energy efficiency tradeoff mechanism towards wireless green communication: A survey. IEEE Communications Surveys and Tutorials. 2016 May;18(1):686-705. https://dx.doi.org/10.1109/COMST.2015.2490540.

[3] Fehske A, Fettweis G, Malmodin J, Biczok G. The global footprint of mobile communications: The ecological and economic perspective. IEEE Communications Magazine. 2011 Aug;49(8). https://dx.doi.org/10.1109/MCOM.2011.5978416.

[4] Prakash S, Baron Y, Liu R, Proske M, Schlossler A. Study on the practical application of the new framework methodology for measuring the environmental impact of ICTCost/benefit analysis. European Commission, Brussels, Studie. 2014. https://dx.doi.org/10.2759/51430.

[5] Han T, Ansari N. Powering mobile networks with green energy. IEEE Wireless Communications. 2014 Feb;21(1):90-6. https://dx.doi.org/10.1109/MWC.2014.6757901.

[6] Chamola V, Sikdar B. Solar powered cellular base stations: Current scenario, issues and proposed solutions. IEEE Communications magazine. 2016 May;54(5):108-14. https://dx.doi.org/10.1109/MCOM.2016.7470944.

[7] Jahid A, Shams AB, Hossain MF. Energy cooperation among BS with hybrid power supply for DPS CoMP based cellular networks. In Electrical, Computer and Telecommunication Engineering (ICECTE), IEEE International Conference on 2016 Dec 8 (pp. 1-4). https://dx.doi.org/10.1109/ICECTE.2016.7879627.

[8] 3GPP, Requirements for further advancements for evolved universal terrestrial radio access (E-UTRA) (LTE-Advanced) (Release 10), TR 36.913, V 10.0.0, 2011.

[9] Svedman P, Wilson SK, Cimini LJ, Ottersten B. Opportunistic beamforming and scheduling for OFDMA systems. IEEE Transactions on Communications. 2007 May;55(5):941-52. https://dx.doi.org/10.1109/ICC.2008.135.

[10] Qamar F, Dimyati KB, Hindia MN, Noordin KA, Al-Samman AM. A comprehensive review on coordinated multi-point operation for LTE-A. Computer Networks. 2017 Aug 4;123:19-37. https://dx.doi.org/10.1016/j.comnet.2017.05.003.

[11] Agrawal R, Bedekar A, Gupta R, Kalyanasundaram S, Kroener H, Natarajan B. Dynamic point selection for LTE-advanced: algorithms and performance. In Wireless Communications and Networking Conference (WCNC), 2014 IEEE 2014 Apr 6 (pp. 1392-1397). https://dx.doi.org/10.1109/WCNC.2014.6952393.

[12] Kaleem Z, Chang K. QoS priority-based coordinated scheduling and hybrid spectrum access for femtocells in dense cooperative 5G cellular networks. Transactions on Emerging Telecommunications Technologies. 2018 Jan; 29(1):1-17. https://dx.doi.org/10.1002/ett.3207.

[13] Huawei White Paper, Improving energy efficiency, Lower CO2 emission and TCO, pp. 1-16, 2011. www.mobilontelecom.com/Huawei-Energy-Efficiency-White-Paper.pdf

[14] Jahid A, Shams AB, Hossain MF. PV-powered CoMP-based green cellular networks with a standby grid supply. International Journal of Photoenergy. Article ID: 6189468. 2017 Apr 4;2017. https://dx.doi.org/10.1155/2017/6189468.

[15] Lorincz J, Matijevic T. Energy-efficiency analyses of heterogeneous macro and micro base station sites. Computers & Electrical Engineering. 2014 Feb 28;40(2):330-49. https://dx.doi.org/10.1016/j.compeleceng.2013.10.013.

[16] Jahid A, Ahmad AS, Hossain MF. Energy efficient BS cooperation in DPS CoMP based cellular networks with hybrid power supply. In Computer and Information Technology (ICCIT), 2016 19th International Conference on 2016 Dec 18 (pp. 93-98). https://dx.doi.org/10.1109/ICCITECHN.2016.7860175.

[17] Ismail M, Zhuang W, Serpedin E, Qaraqe K. A survey on green mobile networking: From the perspectives of network operators and mobile users. IEEE Communications Surveys & Tutorials. 2015 Aug;17(3):1535-56. https://dx.doi.org/10.1109/COMST.2014.2367592.

[18] Liu D, Chen Y, Chai KK, Zhang T, Elkashlan M. Two-dimensional optimization on user association and green energy allocation for HetNets with hybrid energy sources. IEEE Transactions on Communications. 2015 Nov;63(11):4111-24. https://dx.doi.org/10.1109/TCOMM.2015.2470659.

[19] Wang B, Yang Q, Yang LT, Zhu C. On minimizing energy consumption cost in green heterogeneous wireless networks. Computer Networks. 2017 Dec 24;129:522-35. https://dx.doi.org/10.1016/j.comnet.2017.03.024.

[20] Huang PH, Sun SS, Liao W. GreenCoMP: Energy-aware cooperation for green cellular networks. IEEE Transactions on Mobile Computing. 2017 Jan 1;16(1):143-57. https://dx.doi.org/10.1109/TMC.2016.2538231.

[21] Jahid A, Shams AB, Hossain MF. Energy efficiency of JT CoMP based green powered LTE-A cellular networks. In Wireless Communications, Signal Processing and Networking (WiSPNET), 2017, IEEE International Conference on 2017 Mar 24 (pp. 1739-45). https://dx.doi.org/10.1109/WiSPNET.2017.8300060.

[22] Xu J, Zhang R. CoMP meets smart grid: A new communication and energy cooperation paradigm. IEEE Transactions on Vehicular Technology. 2015 Jun;64(6):2476-88. https://dx.doi.org/10.1109/TVT.2014.2345415.

[23] Shams AB, Jahid A, Hossain MF. A CoMP based LTE-A simulator for green communications. In Wireless Communications, Signal Processing and Networking (WiSPNET), 2017, IEEE International Conference on 2017 Mar 24 (pp. 1751-56). https://dx.doi.org/10.1109/WiSPNET.2017.8300062.

[24] System Advisor Model (SAM). [Online]. Available: https://sam.nrel.gov/

[25] Holtkamp H, Auer G, Bazzi S, Haas H. Minimizing base station power consumption. IEEE Journal on Selected Areas in Communications. 2014 Feb;32(2):297-306. https://dx.doi.org/10.1109/JSAC.2014.141210